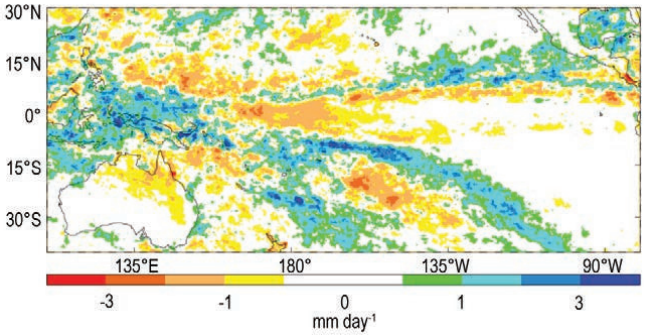

Fig. 4.31. TRMM-3B43 annual average precipitation anomaly (mm day^{-1}) for 2013 with respect to the 1998–2012 average.

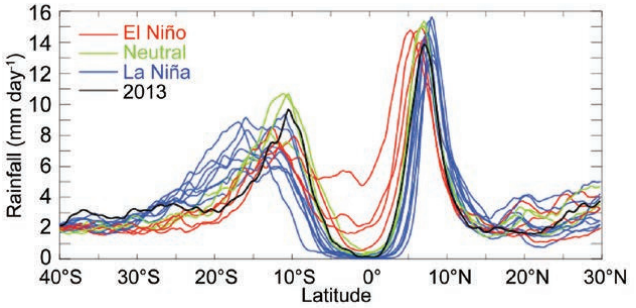

Fig. 4.32. TRMM-3B43 rainfall rate (mm day^{-1}) for Oct–Dec period for each year 1998 to 2013, averaged over the longitude sector 180°–150°W. The cross-sections are color coded by ENSO phase according to NOAA's ONI, except for 2013 (ENSO-neutral) shown in black.

In the westernmost monsoon-dominated sector of Fig. 4.30 (120°–150°E), some pronounced seasonal rainfall anomalies occur. In the southern monsoon period of January–March 2013 (Fig. 4.30a), rainfall did not penetrate as far south as usual, producing substantial dry conditions south of about 13°S (northeastern Australia). During July–September (Fig. 4.30c), rainfall over the Maritime Continent region was enhanced by about 30% over its climatological value between about 5°N and 5°S. The wetter conditions coincided with higher-than-usual SSTs around Indonesia and the Philippines. In September, an active period of TC formation began, culminating in Super Typhoon Haiyan in November.

The SPCZ exhibited generally higher rainfall intensities than normal, especially in the second half of 2013 (180°–150°W sector in Figs. 4.30c,d, and Fig. 4.31). Figure 4.31 also shows that SPCZ convection was particularly vigorous along 10°S east of the dateline. However, the convective activity seemed to split into two parts to the east of Fiji. Rainfall was above normal for the year over and south-southeast of Fiji (18°S, 175°E), but south of 15°S and east of about 160°W there was an extensive drier-than-normal region. This set-up caused strong contrasts in rainfall across the South Pacific Islands. Thus, Tonga (10° east of Fiji) and the Marquesas Islands in the northern part of French Polynesia were generally wetter than normal through much of 2013, whereas many dry months were experienced in central and southern French Polynesia (http://www.niwa.co.nz/climate/icu).

Figure 4.30d for the 180°–150°W sector also suggests that the SPCZ during October–December was equatorward of its normal position, which seems surprising for an ENSO-neutral season. Figure 4.32, which shows south–north rainfall transects for each of the 16 years available from TRMM archive, clarifies the interpretation. In this season, the latitude of the SPCZ rainfall peak tends to be similar in both ENSO-neutral and El Niño years, although rainfall decreases more sharply poleward of this maximum during El Niño years; however, La Niña years have the peak rainfall displaced significantly poleward, and so drag the climatological peak southwards as well. Thus, Fig. 4.32 shows both ITCZ and SPCZ peak rainfalls align well with the observed locations of other ENSO-neutral years.

2) Atlantic—A. B. Pezza and C. A. S. Coelho

The Atlantic ITCZ is a well-organized convective band that oscillates approximately between 5°–12°N during July–November and 5°N–5°S during January–May (Waliser and Gautier 1993; Nobre and Shukla 1996). Equatorial Kelvin waves can modulate the ITCZ interannual variability and ENSO is also known to influence it on the seasonal time scale (Münnich and Neelin 2005). In 2013, the prevailing scenario was that of weak negative sea surface temperature anomalies in the equatorial Pacific near the South American coast associated with neutral ENSO conditions, with no clear teleconnective forcing driving the behavior of the Atlantic ITCZ (Fig. 4.33). However, the intraseasonal activity within the Atlantic sector responded to the typical "seesaw" mechanism between the hemispheres in terms of water temperature and anomalous horizontal divergence, as exemplified in March by an ITCZ well to the north of its climatological position (following the warm water in the North Atlantic) and corresponding suppressed convection on the eastern Amazon and northeastern Brazil (Figs. 4.34, 4.35).

Based on the local influences outlined above, the year could be divided into January–May as a predominantly dry period in the eastern Amazon and northeastern Brazil, and into June–December as a moderately wet period (Fig. 4.34a,b). In June/July, the positive anomalies to the north of the equator

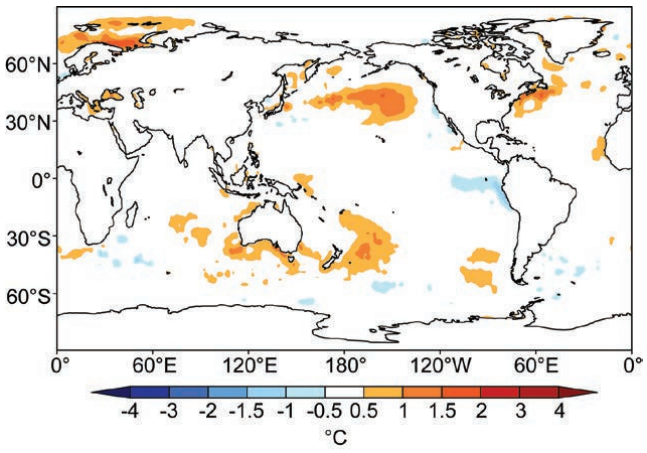

Fig. 4.33. Spatial distribution of average global sea surface temperature anomalies (°C, Reynolds et al. 2002) during 2013.

somewhat dissipated (see the partial reversal of the Atlantic Index, Fig. 4.35b), reducing the subsidence forcing on the Brazilian coast and hence helping explain the more favorable rainfall pattern in the second half of the year. The historical interplay of the SST gradient between the South and the North Atlantic is well depicted by the aforementioned Atlantic Index (Fig. 4.35b), which shows a predominance of negative conditions (unfavorable for convection within the South Atlantic ITCZ) over the last few years.

h. Atlantic warm pool—C. Wang

The Atlantic warm pool (AWP) is a large body of warm water in the lower latitudes of the North Atlantic Ocean, comprising the Gulf of Mexico, the Caribbean Sea, and the western tropical North Atlantic (Wang and Enfield 2001, 2003). Previous studies have shown that the AWP plays an important role in Atlantic TC activity, and provides a moisture source for North America, and thus affects rainfall

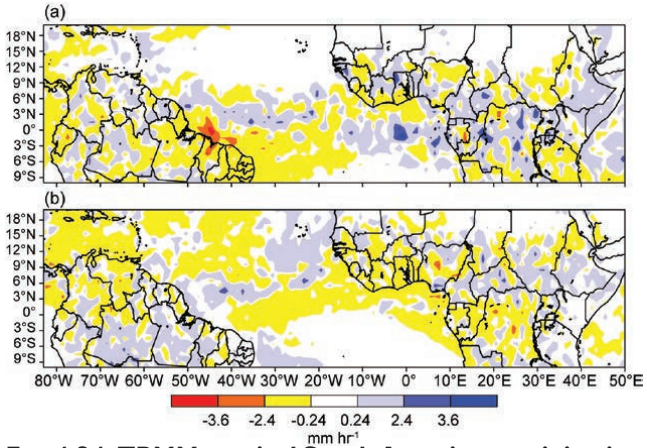

Fig. 4.34. TRMM tropical South America precipitation anomalies (mm hr^{-1}) with respect to 1998–2012 for (a) Jan–May 2013 and (b) Jun–Dec 2013.

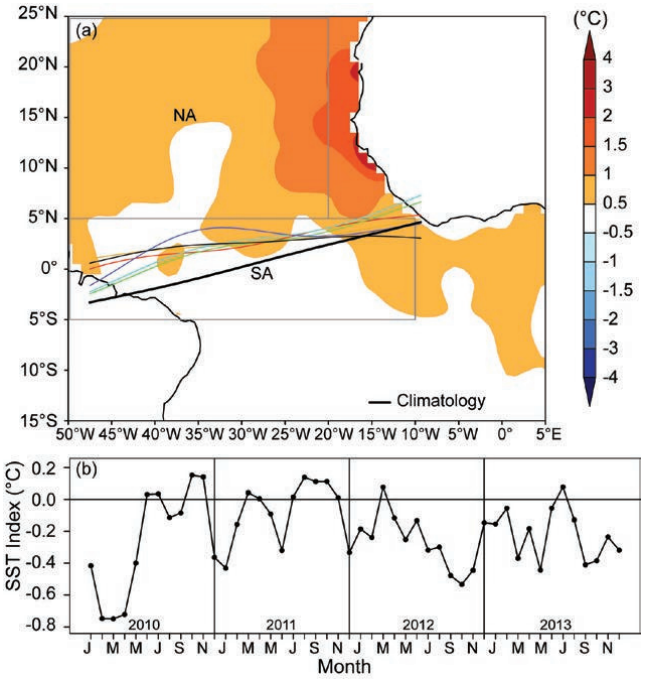

Fig. 4.35. (a) Atlantic ITCZ position inferred from outgoing longwave radiation during Mar 2013. The colored thin lines indicate the approximate position for the six pentads of Mar 2013. The black thick line indicates the Atlantic ITCZ climatological position. The SST anomalies (Reynolds et al. 2002) for Mar 2013 based on the 1982–2012 climatology are shaded. The two boxes indicate the areas used for the calculation of the Atlantic Index in 4.35b; (b) Monthly SST anomaly time series averaged over the South American sector (SA region, 5°S–5°N, 10°–50°W) minus the SST anomaly time series averaged over the North Atlantic sector (NA region, 5°–25°N, 20°–50°W) for the period 2010–13 forming the Atlantic Index. The positive phase of the index indicates favorable conditions for enhanced Atlantic ITCZ activity.

in the central United States (Wang et al. 2006, 2008a, 2011; Drumond et al. 2011). Unlike the Indo-Pacific warm pool, which straddles the equator, the AWP is normally north of the equator. Another unique feature of the AWP is that it does not exist in the boreal winter if the AWP is defined by SSTs warmer than 28.5°C (Wang and Enfield 2001). In addition to the large seasonal cycle, AWP variability occurs on both interannual and multidecadal timescales and has exhibited a long-term warming trend (Wang et al. 2006, 2008b). Figures 4.36a,b depict the long-term total and detrended June–November (JJASON) AWP area indices. The multidecadal and interannual variations of the AWP are displayed in Figs. 4.36c,d respectively.

The multidecadal variability (Fig. 4.36c) shows that the AWPs were larger during the period 1930–60, as well as after the late 1990s; and smaller during 1905–25 and 1965–95. The periods for large and small